

Interstellar Shock Waves

Mark Wardle

**Department of Physics
Macquarie University**

Outline

Shock waves

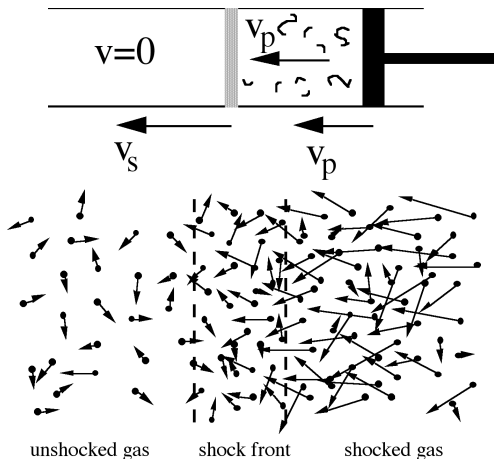
Jump conditions and radiative shocks

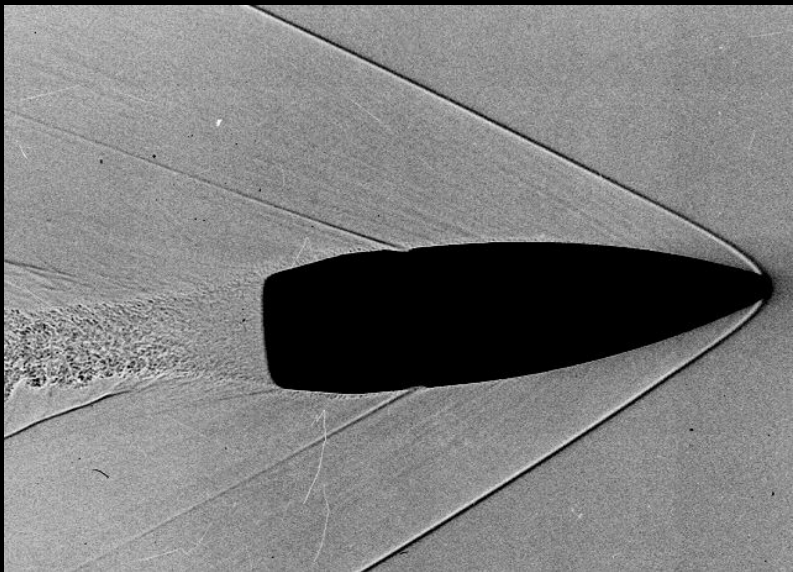
1D steady shock models

Simulations

Shock waves

- Rapid motion: fluid cannot move away until overrun by a disturbance
- Scattering converts unshocked gas to shocked gas
 - compresses and heats gas
 - entropy is increased









Astrophysical shock waves

- Cosmic violence: shock waves are common

$$\text{sound speed: } c_s = \sqrt{\frac{kT}{m}} \approx 3 \text{ km/s} \times \left(\frac{T/1000 \text{ K}}{m/m_p} \right)^{1/2}$$

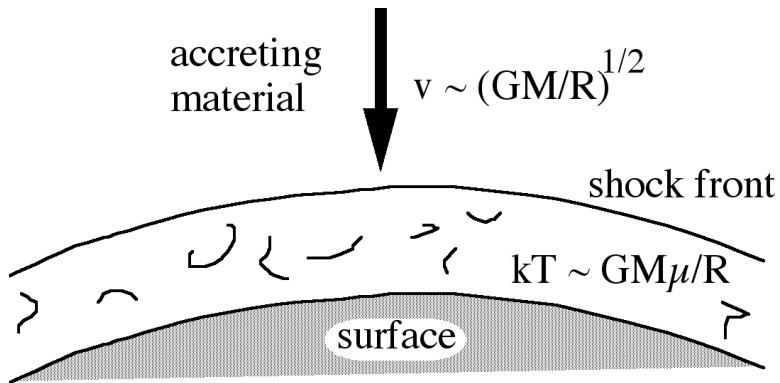
$$\text{Alfvén speed: } v_A = \frac{B}{\sqrt{4\pi\rho}} \approx 2 \text{ km/s} \times \frac{B/\mu\text{G}}{(n_{\text{H}}/\text{cm}^{-3})^{1/2}}$$

- stellar winds, cloud collisions, supernovae, accretion, jets, ...

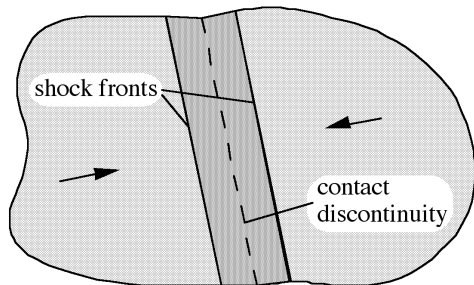
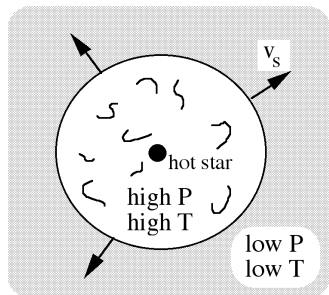
- Shock waves process the gas

- change density, velocity and temperature
- affect ionization state, destroy dust grains, drive chemistry
- introduce structure into the fluid
- particle acceleration
- shocked gas radiates!

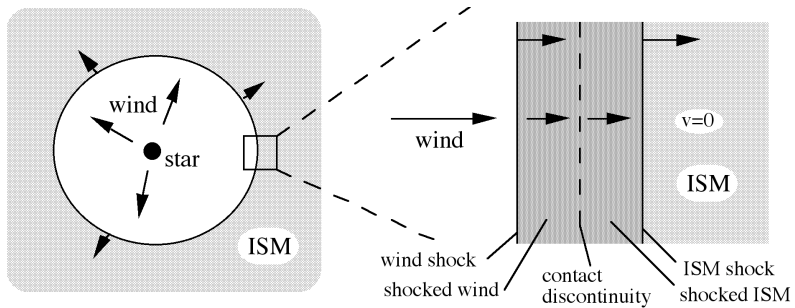
Accretion



Compact HII region / cloud collisions



Stellar wind

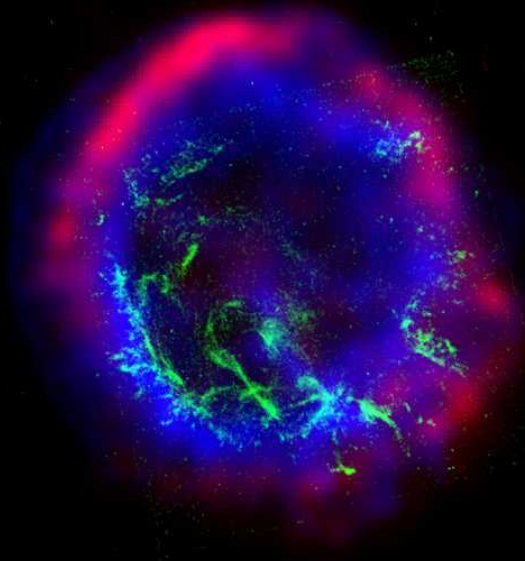




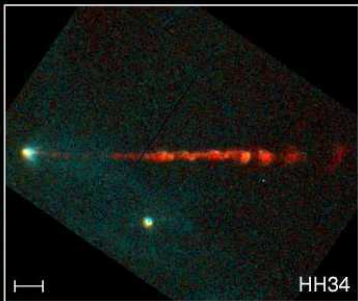
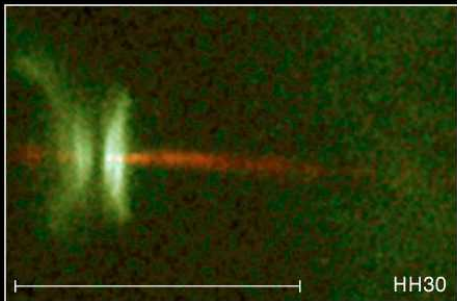
IC 443 supernova remnant



IC 443 – 2MASS

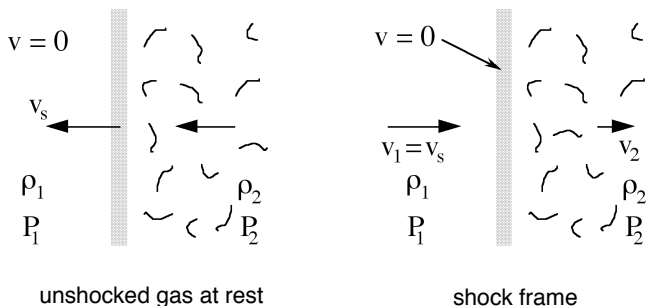


SNR E0102-72



Protostellar jets

Jump Conditions



unshocked gas at rest

shock frame

- Conservation of mass, momentum and energy fluxes across shock front

$$\begin{aligned}
 & \rho v \\
 & \rho v^2 + P + \frac{B^2}{8\pi} \\
 & \left(\frac{1}{2} \rho v^2 + \frac{\gamma P}{\gamma - 1} + \frac{B^2}{4\pi} \right) v \\
 & Bv
 \end{aligned}$$

Strong shocks

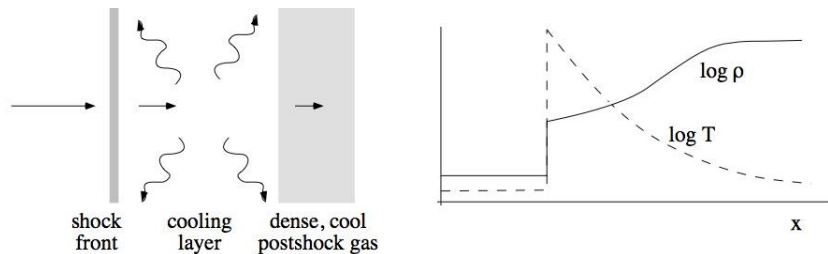
- For $v_s \gg v_A$, c_s and $\gamma > 1$ the jump conditions reduce to

$$\frac{\rho_2}{\rho_1} = \frac{B_2}{B_1} = \frac{v_1}{v_2} \approx \frac{\gamma+1}{\gamma-1} = 4 \quad (\text{for } \gamma = 5/3)$$

$$T_2 \approx \frac{3}{16} \frac{mv_s^2}{k} \approx 1.4 \times 10^5 \left(\frac{v_s}{100 \text{ km/s}} \right)^2 \text{ K}$$

- Magnetic fields hardly affect the jump
 - but if the gas is ionised, their presence leads to particle acceleration which *can* significantly increase the compression ratio
 - and limits the compression of the gas as it cools
 - you have been warned

Radiative shocks



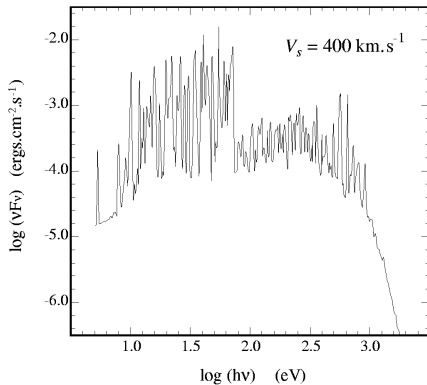
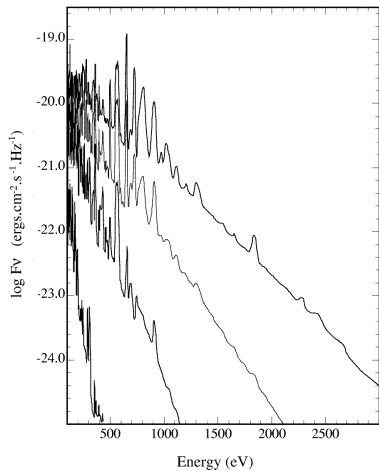
- Shocked gas radiates away energy, so T drops
- Total pressure, $P + B^2/8\pi$ is constant in the postshock gas
- Initially, thermal pressure dominates magnetic pressure
 - ρ increases to compensate for drop in T
 - $B^2/8\pi$ increases as ρ^2
- Magnetic pressure kicks in and halts further compression
 - cool gas forms a dense layer

$$\frac{B^2}{8\pi} \approx \rho_1 v_s^2 \quad \Rightarrow \quad \frac{\rho}{\rho_1} \approx \frac{\sqrt{2} v_s}{v_A} \gg 1$$

Steady, 1D shock models

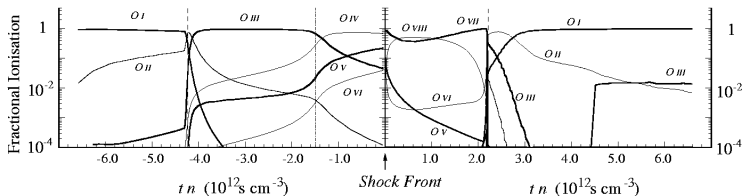
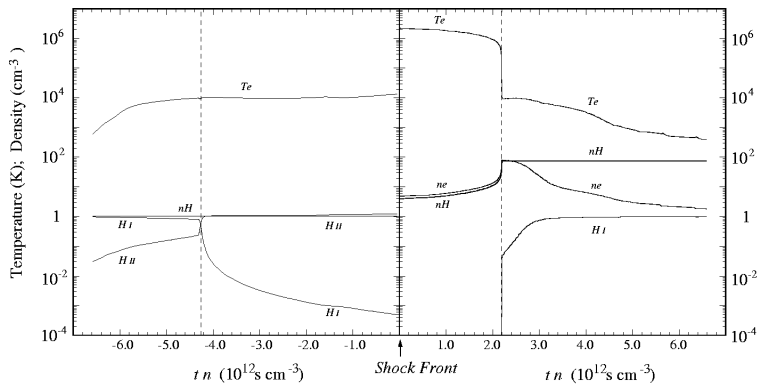
- Follow a fluid element as it passes through the shock and drifts downstream
 - ρ, v, T, B
 - dissociation, ionisation, recombination, chemistry
 - cooling function $\Lambda(\rho, T)$
 - internal excitation: level populations
- A set of ordinary differential equations describe structure of shocked gas
 - local effects only: integrate an initial value problem
 - for $v_s > 100$ km/s, shock-generated radiation gives rise to non-local coupling: iterative methods
 - “trivial” problem compared to fluid simulations
- When does the structure of the shock front matter?
 - particle acceleration in collisionless shocks
 - $v_s < 45$ km/s shocks in molecular clouds (*C-type* shocks)

Atomic shocks

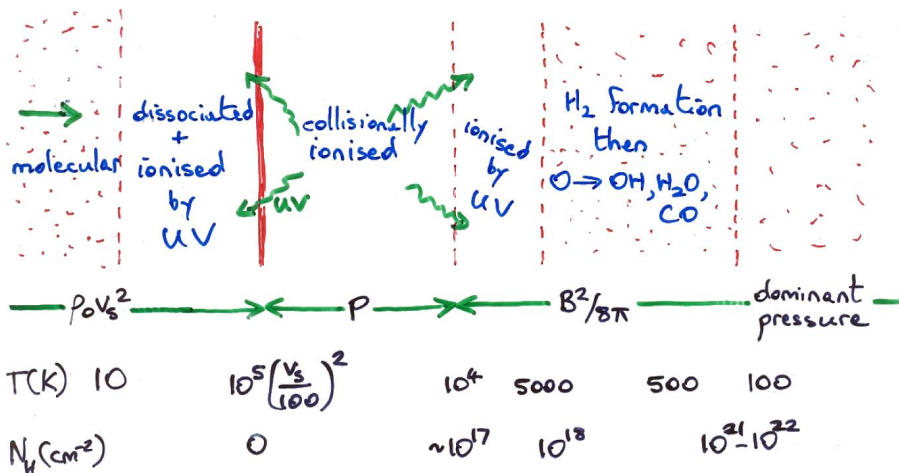


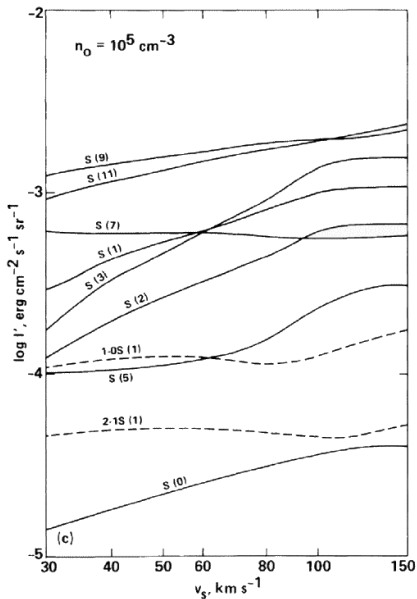
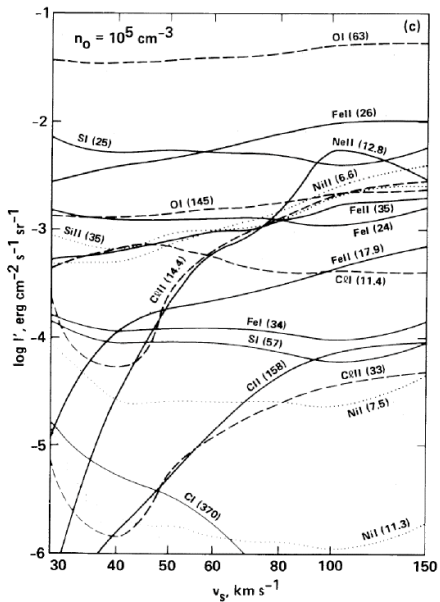
Sutherland & Dopita 1996

Atomic shock - structure



J-type shocks in molecular clouds





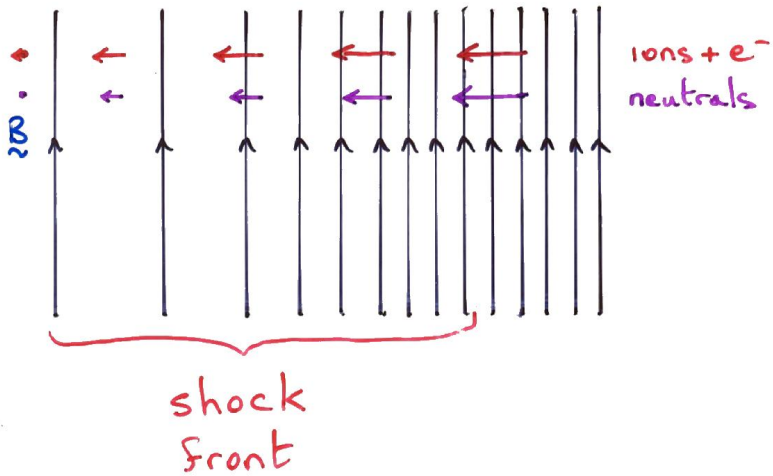
Hollenbach & Mckee 1989

C-type shock waves in molecular clouds

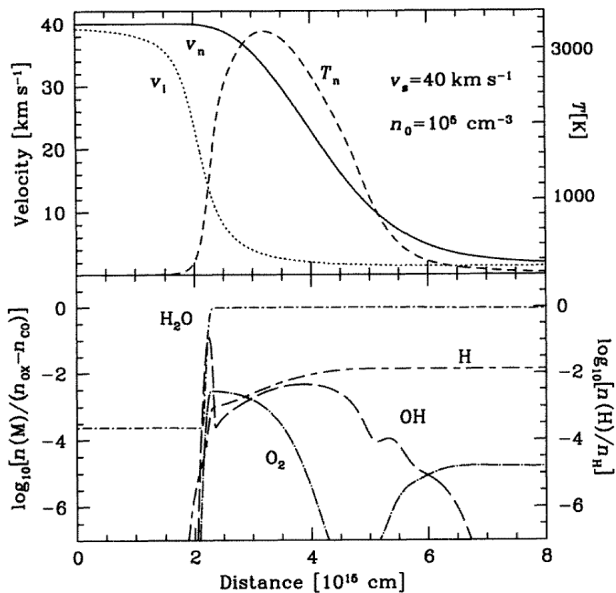
- Molecular clouds are strongly magnetised
 - magnetic pressure ~ 100 times the gas pressure
 - $v_A \approx 2$ km/s, $c_s \approx 0.2$ km/s
- Molecular clouds are weakly ionised
 - cosmic-ray ionisation vs recombination: $n_e \sim 10^{-7} n(\text{H}_2)$:
- Magnetic fields only act on charged particles
 - forces charged particles to drift through the neutrals
 - collisions communicate magnetic forces to the neutral gas:

$$\frac{\mathbf{J} \times \mathbf{B}}{c} = \alpha \rho \rho_i \mathbf{v}_i$$

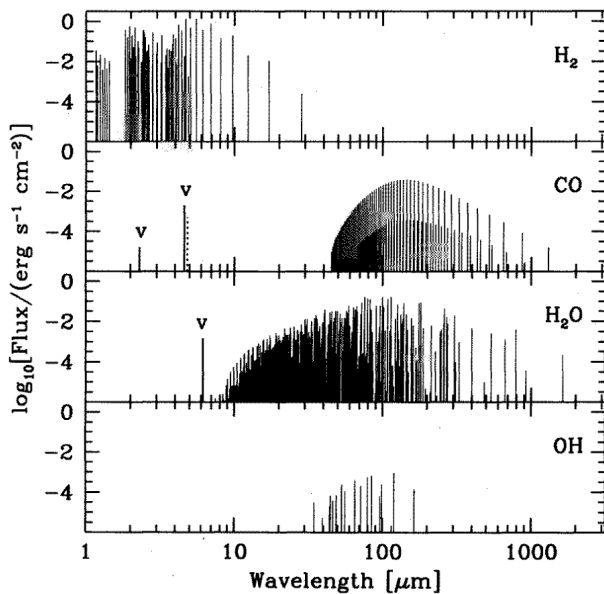
- “ambipolar diffusion”



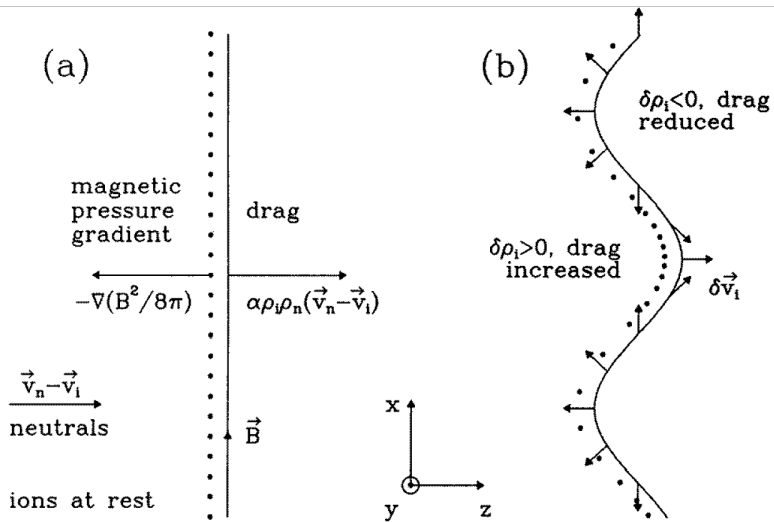
C-shock structure



Line emission

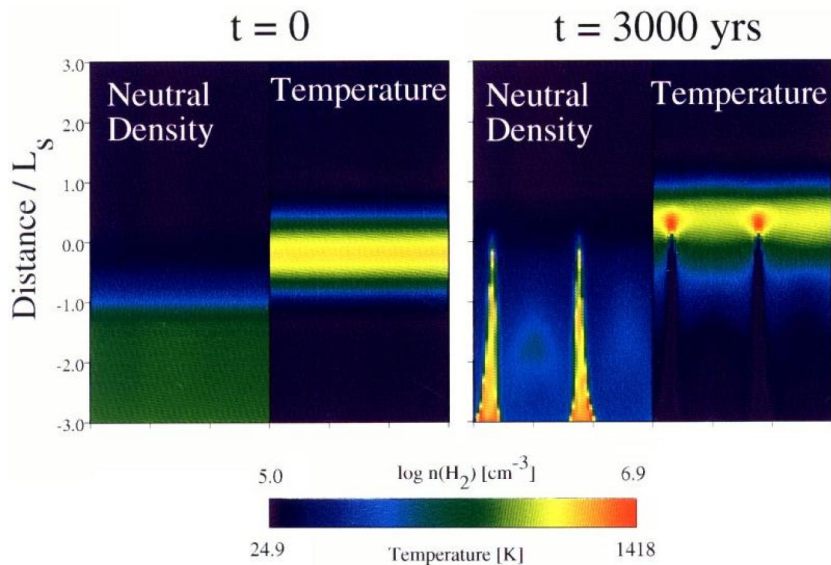


Instability



Wardle 1990

Saturated state (2D)



Neufeld & Stone 1997

Thermal instability

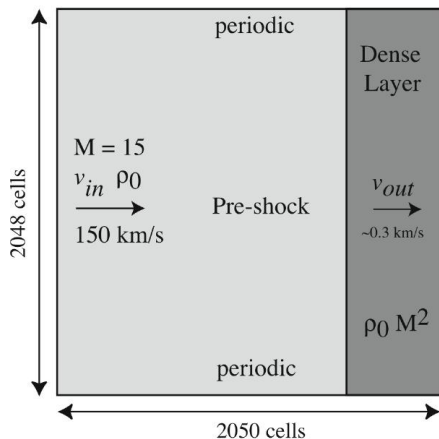


FIG. 11.—Grid setup: the grid size is 2050×2048 cells, 2.0×10^{17} cm on a side. There is a hypersonic inflow on the left at 150 km s^{-1} and subsonic outflow on the right of about 0.3 km s^{-1} , tuned to keep the thickness of the dense layer approximately constant. The y -axis has periodic boundary conditions, approximating an infinite wall shock.

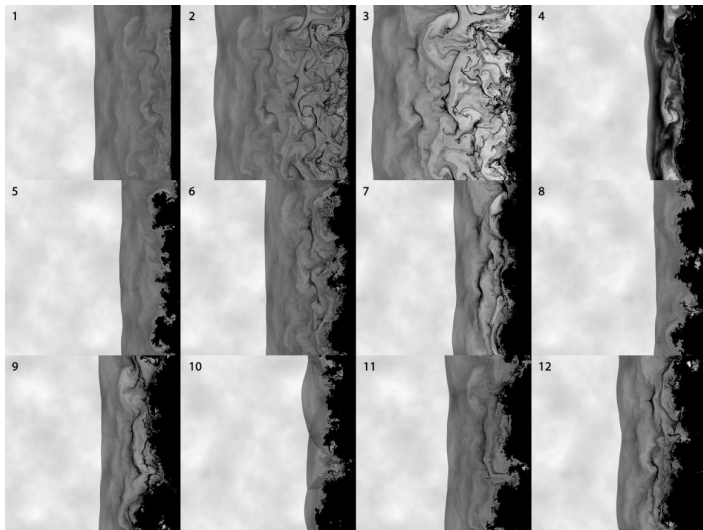


FIG. 12.—Two-dimensional shock time-evolution snapshots. Panels 1–12 show the density variable in the power-law density spectrum shock model at evenly spaced time intervals (2×10^{10} s) throughout the simulation. The postshock gas is at times relatively smooth (1, 5, 8, 10), during the approximately adiabatic buildup of the shock before cooling initiated collapse occurs. The visible fluctuations result from shock compressed initial fluctuations. Subsequently, (2, 6, 9), the fluctuation contrast increases and dense filaments form (3, 7) along with low-density voids. The shock then collapses with the loss of internal pressure support (4).

Shocks hitting clouds

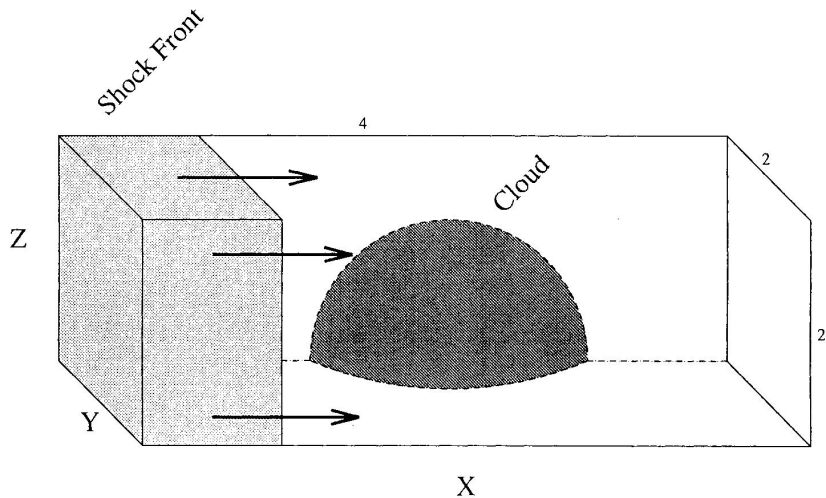
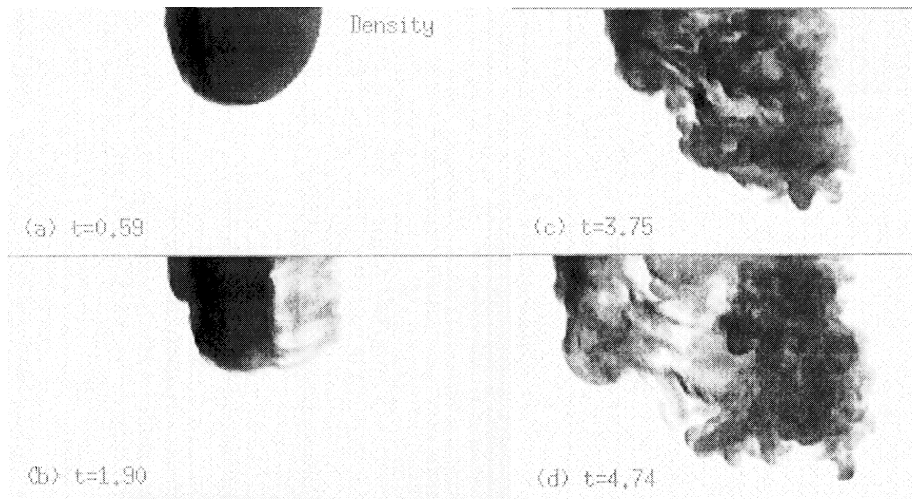


FIG. 1.—A schematic diagram of the problem setup for a spherical cloud

Xu & Stone 1995

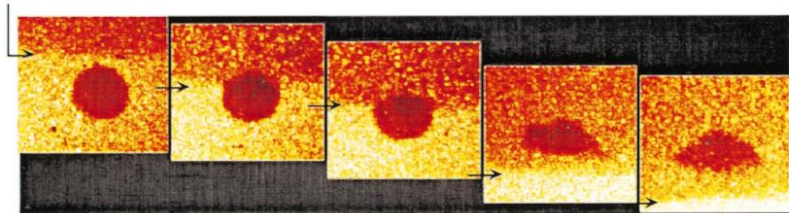
3D



Xu & Stone 1995

NOVA experiments

Shock Position



Distance Down Shock Tube

Klein et al 2003

2D vs 3D

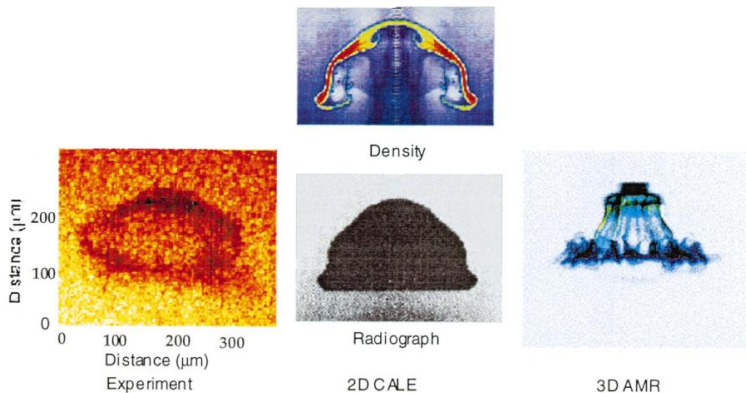


FIG. 3.—A comparison of the experimental radiograph of the sphere (*left*) taken at three crushing times with two-dimensional (*middle*), and three-dimensional (*right*) AMR calculations. The middle panel shows the two-dimensional CALE theoretical radiograph (*bottom*) and a two-dimensional isodensity image (*top*) on the same spatial scale as the experimental radiograph. The bifurcation in the sphere seen in the experiment occurs only with the three-dimensional calculation. The three-dimensional AMR calculations with ideal EOS are scale-free and are meant to show the breakup of the sphere due to vortex ring instabilities.

3D AMR

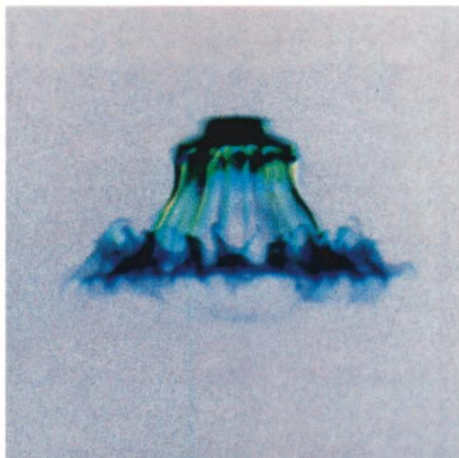
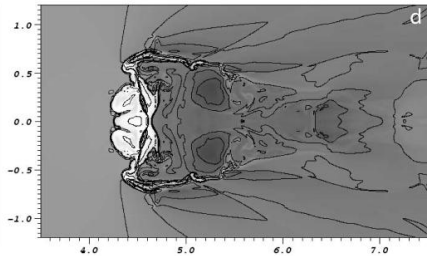
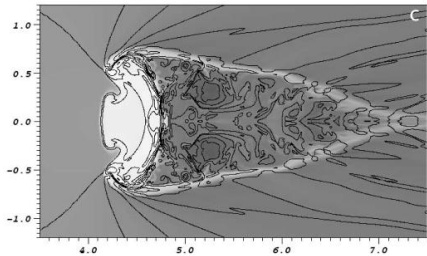
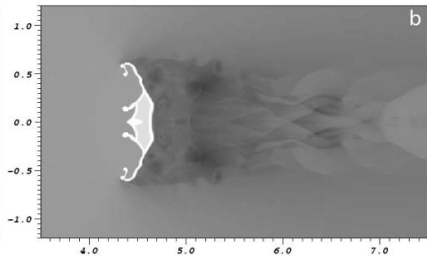
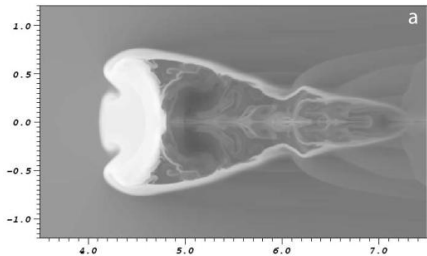
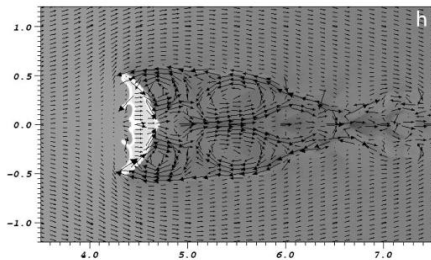
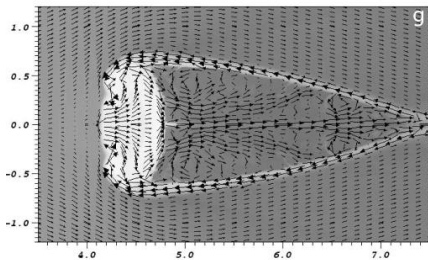
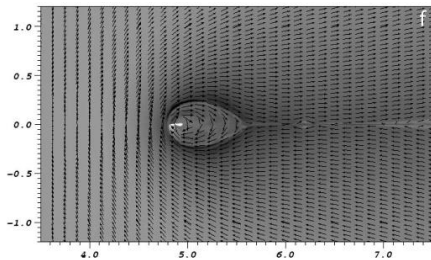
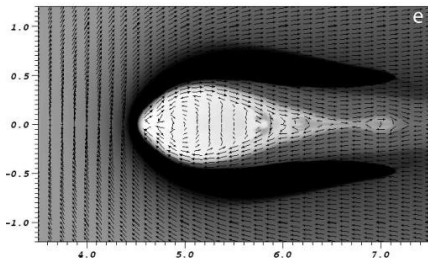


FIG. 19.—Volume-rendered image of three-dimensional AMR simulation of the shocked sphere at late time ($\sim 3t_{\infty}$). The shock originates from the top and moves down. An ideal equation of state and scale-free calculation was used. It shows the breakup of the sphere due to vortex ring instabilities. Note the bifurcation of the sphere and the multimode fluted structure. This unstable lower ringlike structure is a consequence of the Widnall instability.

2D Cartesian with B



Fragile et al 2005



Fragile et al 2005

Summary

- Shock simulations: what should you worry about?
 - Adiabatic vs radiative
 - Magnetohydrodynamics vs hydrodynamics
 - Dimensionality
 - Geometry
 - Boundary conditions
- If you are involved with large-scale simulations that contain shocks what should you be *really* worried about?
 - small-scale shock instabilities
 - subtle aspects of MHD